



HAL
open science

Trajectory tracking for autonomous underwater vehicle: An adaptive approach

Jesus Guerrero, Jorge Torres, Vincent Creuze, Ahmed Chemori

► To cite this version:

Jesus Guerrero, Jorge Torres, Vincent Creuze, Ahmed Chemori. Trajectory tracking for autonomous underwater vehicle: An adaptive approach. *Ocean Engineering*, 2019, 172, pp.511-522. <10.1016/j.oceaneng.2018.12.027>. <lirmm-01970636>

HAL Id: lirmm-01970636

<https://hal-lirmm.ccsd.cnrs.fr/lirmm-01970636v1>

Submitted on 5 Jan 2019

HAL is a multi-disciplinary open access archive for the deposit and dissemination of scientific research documents, whether they are published or not. The documents may come from teaching and research institutions in France or abroad, or from public or private research centers.

L'archive ouverte pluridisciplinaire HAL, est destinée au dépôt et à la diffusion de documents scientifiques de niveau recherche, publiés ou non, émanant des établissements d'enseignement et de recherche français ou étrangers, des laboratoires publics ou privés.



HAL Authorization

Autonomous Underwater Vehicle Trajectory Tracking: An adaptive approach

J. Guerrero^a, J. Torres^a, V. Creuze^b, A. Chemori^b

^a*Automatic Control Department, CINVESTAV, Mexico CDMX, Mexico*

^b*LIRMM, CNRS-Universit Montpellier 2, Montpellier, France*

Abstract

During sea missions, underwater vehicles are exposed to changes in the parameters of the system and subject to persistent external disturbances due to the ocean current influence. These issues make the design of a robust controller a quite challenging task. This paper focuses on the design of an adaptive high order sliding mode control for trajectory tracking on an underwater vehicle. The main feature of the developed control law is that it preserves the advantages of robust control, it does not need the knowledge of the upper bound of the disturbance and easy tuning in real applications. Using Lyapunov concept, asymptotic stability of the closed-loop tracking system is ensured. The effectiveness and robustness of the proposed controller for trajectory tracking in depth and yaw dynamics are demonstrated through real-time experiments.

Keywords: Adaptive control, Underwater Vehicles, Sliding Mode Control, Real-Time Experiments

1. Introduction

Although the oceans cover 70% of the Earth's surface, almost the 95% of the ocean remains unexplored according to data from the National Oceanic and Atmospheric Administration. Recently, underwater robotics has positioned itself as one of the essential areas within maritime exploration due to a long list of advantages as operational efficiency, mobility, and low operational cost [1].

Email address: `jguerrero@ctrl.cinvestav.mx` (J. Guerrero)

8 There are two main classes of underwater vehicles: The Remotely Oper-
9 ated Vehicles (ROVs), which require human piloting and the Autonomous
10 Underwater Vehicles (AUVs), that refer to the submarines able to perform
11 some tasks with full autonomy. A controller provides this autonomy required
12 to position the vehicle at a specific point or to track a path. However, the
13 design of the controller for an AUV is very challenging due to the nonlinear-
14 ity, time-variance, random external disturbances, such as the environmental
15 force generated by the sea's current fluctuation, and the difficulty in accu-
16 rately modeling the hydrodynamic effect [2]. For these reasons, in recent
17 years, different control techniques have been introduced for AUVs.

18 The Proportional-Derivative (PD) [3], the PD plus gravity and buoyancy
19 compensation (PD+) [4, 5] and the Proportional Integral Derivative (PID)
20 schemes are the most used techniques to control the position and orientation
21 of commercial AUVs due to their design simplicity and their good perfor-
22 mance. However, these controllers have some drawbacks. In one hand, the
23 PD+ controller requires the exact knowledge of the gravitational and buoy-
24 ancy force of the robot. On the other hand, it is well-known that the PID
25 control performance is degraded when the plant is highly nonlinear, time-
26 varying, or with significant time delays. Moreover, the listed controllers
27 considering strong restrictive assumptions to simplify the mathematical de-
28 scription, resulting in an impractical controller due to its low robustness
29 against disturbances. For this reason, many researchers concentrated their
30 interests on the applications of robust control for underwater vehicles.

31 A broad class of robust controllers has been proposed for the trajec-
32 tory tracking problem on AUV. For example, Fuzzy Logic Controllers (FLC)
33 [6] [7], Neural-Network based control (NNC) [8, 9], Predictive control [10],
34 Adaptive control [11], Sliding Modes Control (SMC) [12], High Order Slid-
35 ing Modes Control (HOSMC) [13, 14] and so on. Each methodology has
36 strengths and weaknesses. For instance, FLC has a simple structure, easy
37 and cost-effective design. However, the controller tuning process might be a
38 bit difficult because there is no stability criterion or FLC cannot be imple-
39 mented for unknown systems.

40 The main advantage of NNC is their ability to learn from examples instead
41 of requiring an algorithmic development from the designer. Nevertheless,
42 NNC usually needs a long and computationally expensive training time which
43 is not acceptable in many applications.

44 Adaptive control covers a set of techniques which provide a systematic
45 approach for automatic adjustment of controllers in real time, in order to

46 achieve or to maintain the desired level of system performance when the
47 parameters of the dynamic model are unknown or change in time [15].

48 Sliding Mode Control (SMC) is another robust technique sometimes used
49 in underwater vehicle control. This technique provides finite time conver-
50 gence and robustness against bounded external disturbances. In its basic
51 implementations, this controller can have aggressive control input behavior
52 due to signum function which causes the undesirable chattering effect. How-
53 ever, there exist several ways to decrease the chattering effect, like replacing
54 the signum function by a hyperbolic tangent, sigmoid or saturation functions
55 [4] which smooths the control signal, but at the cost of loss of robustness
56 because it constrains the sliding systems trajectories to the sliding surface's
57 vicinity [16]. High Order Sliding Mode Control (HOSMC) is another conven-
58 tional technique to reduce the chattering amplitude. This methodology takes
59 advantage of quasi-continuous control which allows driving to the origin the
60 sliding surface and its derivative in the presence of external disturbances. Fi-
61 nally, SMC with auto-adjustable [17] or dynamical gains [18] is an alternative
62 solution to minimize the impact of the first order SMC drawbacks. In these
63 techniques, an adaptive law is proposed to adjust the feedback controller
64 gains according to the disturbance impact. There are many works following
65 this philosophy. For instance, an adaptive first-order SMC for the set-point
66 stabilization of an AUV is proposed in [19]. In this work, the control signal
67 was divided into three terms: first, the equivalent control term to neglect the
68 known parameters of the system. Second, the discontinuous signum function
69 which minimizes the disturbance impact. Finally, the adaptive part which
70 allows adjusting the feedback controller gains without the prior knowledge
71 of the disturbance's bounds. In [20] an adaptive SMC for the trajectory
72 tracking of pitch and yaw dynamics is proposed. In the design of the con-
73 troller, it is taken into account the actuator's non-symmetric dead-zones and
74 unknown disturbances. The adaptive law and the disturbance observer were
75 designed to adjust the controller's gains while an anti-windup compensator
76 was introduced to prevent actuator's saturation. Simulation and experimen-
77 tal results demonstrate the effectiveness of the proposed methodology. Also,
78 an adaptive SMC for depth trajectory tracking of a ROV taking into account
79 thruster's saturation and dead-zones is proposed in [21]. A three-layer feed-
80 forward neural network was used to identify unknown model parameters and
81 adaptive laws to estimate the algorithm gains. Simulation results validate
82 the correct behavior of the proposed method.

83 An adaptive second-order SMC for depth and yaw path following is pro-

84 posed in [22]. A nonlinear function was introduced into the sliding surface
85 to modify the damping ratio of the controller output. Then, the gain of
86 the controller is estimated through the adaptive law which needs the distur-
87 bance's upper bound information. The efficiency of the proposed controller is
88 demonstrated through real-time experiments. In [23], a multi-variable output
89 feedback adaptive nonsingular terminal SMC for the four degrees of freedom
90 trajectory tracking of AUV was developed. In this work, an adaptive ob-
91 server with equivalent output injection was designed in order to estimate
92 the system's states in finite time while the adaption control law stabilize the
93 trajectory tracking error to a small field in finite time. Through computer
94 simulations, the effectiveness of proposed controller was highlighted com-
95 pared against similar methodologies. Also, in [24], an adaptive second-order
96 fast nonsingular terminal SMC for AUV is proposed. In this work, the prior
97 information about the upper bound of the disturbance is not required. Based
98 on simulation results, chattering reduction and fast convergence is demon-
99 strated when parameter uncertainties of 20 % and time variant disturbances
100 were considered. In [25], an adaptive integral SMC for AUV stabilization was
101 proposed. In this paper, two scenarios were considered. In the first case, it
102 is assumed that the full system parameters were not available. In the second
103 one, it is supposed that the system is affected by external disturbances. In
104 both cases, the proposed adaptive law adjust the feedback controller gains
105 in order to suppress the chattering effect.

106 In this context, the adaptive version of the well-known Super-Twisting
107 (STW) controller is proposed in [18]. The STW algorithm was introduced
108 initially in [26] ensures robustness with respect to parametric uncertainties
109 and external disturbances while reducing the chattering effect. However,
110 the main drawback of this method is that is necessary the knowledge of the
111 boundaries of the disturbance gradients. In the mentioned adaptive version,
112 the algorithm does not require any information on the bounds of the distur-
113 bance and its gradient. The method was developed for a single-input uncer-
114 tain nonlinear system. Based on real-time experiments, the authors prove
115 the good performance of the adaptive algorithm on the position control of
116 an electro-pneumatic actuator.

117 In this paper, based on the previous results of [27] and [18], an adaptive
118 high order sliding mode control for trajectory tracking of an AUV is devel-
119 oped. In this case, taking into account the procedure shown in the cited
120 papers, the adaption law is applied to the Generalized Super-Twisting Al-
121 gorithm (GSTA) which compared to the STW, the GSTA includes a linear

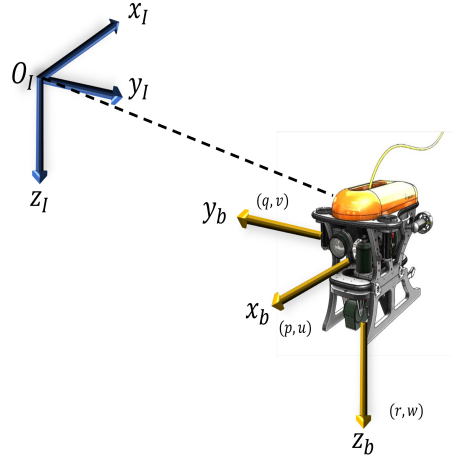


Figure 1: Underwater vehicle with the inertial-fixed frame (O_I, x_I, y_I, z_I) and the body-fixed frame (O_b, x_b, y_b, z_b) .

122 version of the algorithm, the standard STA, and a STA with extra linear cor-
 123 rection terms, that provide more robustness and convergence velocity [28].
 124 The GSTA as well the STW, requires the knowledge of the bounds of the
 125 disturbance gradient. However, applying the adaptive law relaxes this condi-
 126 tion, and the algorithm does not require it. Lyapunov arguments prove the
 127 stability of the proposed controller. Real-time experiments in depth and yaw
 128 trajectory tracking for an underwater vehicle demonstrate the effectiveness
 129 of the proposed method.

130 The remainder of this paper is organized as follows: The underwater ve-
 131 hicle dynamics equation is derived in Section 2. In Section 3, an adaptive
 132 high order sliding mode controller for trajectory tracking and its stability
 133 analysis is presented. In order to demonstrate the effectiveness of the pro-
 134 posed control scheme, real-time experiments for yaw and depth trajectory
 135 tracking tests for several scenarios are presented in Section 5. Finally, we
 136 make a brief conclusion on the paper in Section 6.

137 2. Dynamic Model

138 The dynamic model of underwater vehicles has been described in several
 139 works (see for instance ([4, 29, 30, 31, 32])).

140 The dynamics of an underwater vehicle involves two frames of reference:
 141 the body-fixed frame and the earth-fixed frame (see Fig. 1). Considering the
 142 generalized inertial forces, the hydrodynamic effects, the gravity and buoy-
 143 ancy contributions as well as the forces of the actuators (i.e., thrusters), the
 144 dynamic model of an underwater vehicle in matrix form, using the SNAME
 145 notation [33] and the representation introduced by [4], can be written as
 146 follows:

$$\begin{aligned} M\dot{\nu} + C(\nu)\nu + D(\nu)\nu + g(\eta) &= \tau + w_e(t) \\ \dot{\eta} &= J(\eta)\nu \end{aligned} \quad (1)$$

147 Where $\nu = [u, v, w, p, q, r]^T$ is the state vector of velocity relative to the
 148 body-fixed frame and $\eta = [x, y, z, \phi, \theta, \psi]^T$ represents the vector of position
 149 and orientation relative to the earth-fixed frame. From equation (1), the
 150 matrix of spatial transformation between the inertial frame and the frame
 151 of the rigid body can be as $J(\eta) \in \mathbb{R}^{6 \times 6}$. $M \in \mathbb{R}^{6 \times 6}$ is the inertia matrix
 152 where the effects of mass are included, $C(\nu) \in \mathbb{R}^{6 \times 6}$ is the Coriolis-centripetal
 153 matrix, $D(\nu) \in \mathbb{R}^{6 \times 6}$ represents the hydrodynamic damping matrix, $g(\eta) \in$
 154 \mathbb{R}^6 is the vector of gravitational/buoyancy forces and moments. Finally,
 155 $\tau \in \mathbb{R}^6$ is the control vector acting on the underwater vehicle and $w_e(t) \in \mathbb{R}^6$
 156 defines the vector of external disturbances.

157 The presented formulation of the AUV dynamics is expressed in the body-
 158 fixed frame and can be transformed to the earth-fixed frame by using the
 159 kinematic transformations of the state variables and the model parameters
 160 as follows:

$$\begin{aligned} M_\eta(\eta) &= J^{-T}(\eta)MJ^{-1}(\eta) \\ C_\eta(\nu, \eta) &= J^{-T}(\eta) \left[C(\nu) - MJ^{-1}(\eta)\dot{J}(\eta) \right] J^{-1}(\eta) \\ D_\eta(\nu, \eta) &= J^{-T}(\eta)D(\nu)J^{-1}(\eta) \\ g_\eta(\eta) &= J^{-T}(\eta)g(\eta) \\ \tau_\eta(\eta) &= J^{-T}(\eta)\tau \\ w_\eta(t) &= J^{-T}(\eta)w_e(t) \end{aligned}$$

Based on these equalities, the dynamics (1) can therefore be rewritten in
 the earth-fixed frame as:

$$\underbrace{M_\eta(\eta)\ddot{\eta} + C_\eta(\nu, \eta)\dot{\eta} + D_\eta(\nu, \eta)\dot{\eta} + g_\eta(\eta)}_{f(\nu, \eta)} = \tau_\eta(\eta) + w_\eta(t) \quad (2)$$

161 Hydrodynamic loads dominate the AUV dynamics, and it is difficult to
 162 accurately measure or estimate the hydrodynamic coefficients that are valid
 163 for all vehicle operating conditions. As such, the system dynamics are not
 164 exactly known. Therefore, the system dynamics $f(\eta, \nu)$ given in (2) can be
 165 written as the sum of estimated dynamics $\hat{f}(\eta, \nu)$ and the unknown dynamics
 166 $\tilde{f}(\eta, \nu)$ as follows:

$$f(\eta, \nu) = \hat{f}(\eta, \nu) + \tilde{f}(\eta, \nu) \quad (3)$$

167 where:

$$\hat{f}(\eta, \nu) = \hat{M}_\eta(\eta)\ddot{\eta} + \hat{C}_\eta(\nu, \eta)\dot{\eta} + \hat{D}_\eta(\nu, \eta)\dot{\eta} + \hat{g}_\eta(\eta) \quad (4)$$

$$\tilde{f}(\eta, \nu) = \tilde{M}_\eta(\eta)\ddot{\eta} + \tilde{C}_\eta(\nu, \eta)\dot{\eta} + \tilde{D}_\eta(\nu, \eta)\dot{\eta} + \tilde{g}_\eta(\eta) \quad (5)$$

168 Moreover, the matrices of the unknown dynamics vector $\tilde{f}(\eta, \nu)$ are de-
 169 fined as $\tilde{M}_\eta = M_\eta - \hat{M}_\eta$, $\tilde{C}_\eta = C_\eta - \hat{C}_\eta$, $\tilde{D}_\eta = D_\eta - \hat{D}_\eta$ and $\tilde{g}_\eta = g_\eta - \hat{g}_\eta$.

170 Rewriting the system (2) into the estimated and unknown dynamics given
 171 by (3), we have:

$$\hat{M}_\eta(\eta)\ddot{\eta} + \hat{C}_\eta(\nu, \eta)\dot{\eta} + \hat{D}_\eta(\nu, \eta)\dot{\eta} + \hat{g}_\eta(\eta) = \tau_\eta(\eta) + \bar{w}(t) \quad (6)$$

172 where $\bar{w}(t) = w_\eta(t) - \tilde{f}(\eta, \nu)$.

173 Finally, note that the dynamical model of the AUV given by (6) only
 174 depends on the estimated values of system parameters shown in Equation
 175 (2).

176 3. Controller Design

177 In this section, the design of an adaptive gain high order sliding mode
 178 control for the AUV is addressed. The controller is based on the General-
 179 ized Super-Twisting Algorithm (GSTA) developed by [28] which is a general
 180 form of the original Super-Twisting Algorithm (STA) introduced by [26]. In-
 181 spired by the methodology presented in [27] where the authors developed an
 182 adaptive control law based on the original STW control for a single-input un-
 183 certain nonlinear system. In this work, we use the GSTA instead of the STA,
 184 and we extend the procedure shown in the cited article to a MIMO non-linear
 185 system such as the mathematical model of the AUV. Finally, the stability of
 186 the proposed controller is proven through Lyapunov function arguments.

187 *3.1. Adaptive GSTA Design*

First, let the next state variables:

$$\chi_1 = \eta \quad ; \quad \chi_2 = \dot{\eta}$$

Rewriting the model (6) as follows:

$$\begin{aligned} \dot{\chi}_1 &= \chi_2 \\ \dot{\chi}_2 &= F(\chi) + G(\chi)\tau_\eta + w(t) \end{aligned} \quad (7)$$

where:

$$\begin{aligned} F(\chi) &= -\hat{M}_\eta(\eta)^{-1} \left[\hat{C}_\eta(\nu, \eta)\dot{\eta} + \hat{D}_\eta(\nu, \eta)\dot{\eta} + \hat{g}_\eta(\eta) \right] \\ G(x) &= \hat{M}_n(\eta)^{-1} J^{-T}(\eta) \\ w(t) &= \hat{M}_\eta(\eta)^{-1} \bar{w}(t) \end{aligned}$$

188 Before introduce the design of the adaptive controller, it is necessary to
189 consider the following assumptions:

190 **Assumption 1.** *The pitch angle is smaller than $\pi/2$, i.e., $|\theta| < \pi/2$.*

191 **Assumption 2.** *The perturbation $w(t)$ is a Lipschitz continuous signal.*

192 According to A1, the inverse of rotational matrix $J(\eta)$ exists. Then, $G(\chi)$ is
193 not singular, therefore, its inverse exists.

194 According to A2, the time derivative of the external disturbance term
195 $w(t)$ is bounded by

$$|\dot{w}_i(t, x)| \leq L_i |\phi_2(\sigma)| \quad , \quad i = \overline{1, 6}. \quad (8)$$

196 with $L_i \geq 0$ is a finite boundary but is not known.

197 From (7) it is possible to propose a sliding surface depending on the error
198 that force the sliding mode in the manifold as follows:

$$\sigma = \dot{e}(t) + \Lambda \cdot e(t) \quad (9)$$

where $\sigma(t) := [\sigma_1, \sigma_2, \dots, \sigma_6]^T$, $e(t) = \chi_1^d(t) - \chi_1(t)$ is the error vector and the desired trajectory is defined as $\chi_1^d(t) = [x_d(t), y_d(t), z_d(t), \phi_d(t), \theta_d(t), \psi_d(t)]^T$. $\dot{e}(t) = \dot{\chi}_2^d(t) - \dot{\chi}_2(t) = \dot{\chi}_1^d(t) - \dot{\chi}_1(t)$ is the time derivative of the error and $\Lambda =$

$diag(\Lambda_1, \Lambda_2, \dots, \Lambda_6) \in \mathbb{R}^{6 \times 6}$ is a diagonal positive definite matrix. Finally, the control law for the underwater vehicle is given as follows:

$$\tau_\eta = J^T \hat{M}_\eta(\eta) [\ddot{\chi}_1^d(t) + \Lambda \dot{e}(t) - F(\chi) - v] \quad (10)$$

where v is the GSTA and is defined by:

$$\begin{aligned} v &= -K_1(t)\Phi_1(\sigma) + \lambda \\ \dot{\lambda} &= -K_2(t)\Phi_2(\tau) \end{aligned} \quad (11)$$

with the vectors $\Phi_1(\sigma) = [\phi_{11}, \phi_{12}, \dots, \phi_{16}]^T$ and $\Phi_2(\tau) = [\phi_{21}, \phi_{22}, \dots, \phi_{26}]^T$ and each element is given by:

$$\begin{aligned} \phi_{1i}(\sigma_i) &= \mu_{1i}|\sigma_i|^{1/2}sgn(\sigma_i) + \mu_{2i}\sigma_i \\ \phi_{2i}(\sigma_i) &= \frac{1}{2}\mu_{1i}^2sgn(\sigma_i) + \frac{3}{2}\mu_{1i}\mu_{2i}|\sigma_i|^{1/2}sgn(\sigma_i) + \mu_{2i}^2\sigma_i \end{aligned}$$

199 where $\mu_{1i}, \mu_{2i} \geq 0$ with $i = \overline{1, 6}$. $K_1(t) = diag(k_{11}(t), k_{12}(t), \dots, k_{16}(t))$ and
 200 $K_2(t) = diag(k_{21}(t), k_{22}(t), \dots, k_{26}(t))$ are the gain matrices which satisfy
 201 $K_1(t) = K_1(t)^T > 0$ and $K_2(t) = K_2(t)^T > 0$.

Moreover, if each element of the controller gain matrices is selected as follows:

$$\dot{k}_{1i}(t) = \begin{cases} \omega_i \sqrt{\varsigma_i} & \text{if } \sigma \neq 0 \\ 0 & \text{if } \sigma = 0 \end{cases} \quad (12)$$

$$k_{2i}(t) = 2\epsilon_i k_{1i}(t) + \beta_i + 4\epsilon_i^2 \quad (13)$$

202 where $\omega_i, \varsigma_i, \beta_i$ and ϵ_i are arbitrary positive constants with $i = \overline{1, 6}$. Then,
 203 for any initial condition $\sigma_i(0)$, the sliding surface $\sigma_i = 0$ will be reached in
 204 finite time.

205 3.2. Stability Analysis

206 **Theorem 1.** *From the underwater vehicle model (2), suppose that the dis-*
 207 *turbance term $w(t)$ satisfies (8). Then for any initial conditions $\chi(0), \sigma(0)$*
 208 *the sliding surface $\sigma = 0$ will be reached in finite time via AGSTA (11) with*
 209 *the adaptive gains selected as shown in equations (12).*

210 **Proof 1.** *Taking into account the underwater vehicle model given by (7),*
 211 *the the control law (10) and the sliding surface dynamics (9), leads to the*
 212 *following closed-loop error dynamics:*

$$\dot{\sigma} = -K_1(t)\Phi_1(\sigma) - K_2(t) \int_0^t \Phi_2(\sigma(\tau))d\tau + w(t) \quad (14)$$

Now, taking the following change of variables:

$$\begin{aligned} s_{1i} &= \sigma_i \\ s_{2i} &= -k_{2i} \int_0^t \phi_{2i}(\sigma_i(\tau)) d\tau + w_i(t) \end{aligned}$$

Then (14) can be rewritten in scalar form ($i = \overline{1, 6}$) as:

$$\begin{aligned} \dot{s}_{1i} &= -k_{1i} \left[\mu_{1i} |s_{1i}|^{\frac{1}{2}} \operatorname{sgn}(s_{1i}) + \mu_{2i} s_{1i} \right] + s_{2i} \\ \dot{s}_{2i} &= -k_{2i} \left[\frac{1}{2} \mu_{1i}^2 \operatorname{sgn}(s_{1i}) + \frac{3}{2} \mu_{1i} \mu_{2i} |s_{1i}|^{\frac{1}{2}} \operatorname{sgn}(s_{1i}) + \mu_{2i}^2 s_{1i} \right] + \frac{d}{dt} w_i(t, \chi) \end{aligned}$$

Without loss of generality, we can represent the system with simplified notation:

$$\begin{aligned} \dot{s}_1 &= -k_1 \left[\mu_1 |s_1|^{\frac{1}{2}} \operatorname{sgn}(s_1) + \mu_2 s_1 \right] + s_2 \\ \dot{s}_2 &= -k_2 \left[\frac{1}{2} \mu_1^2 \operatorname{sgn}(s_1) + \frac{3}{2} \mu_1 \mu_2 |s_1|^{\frac{1}{2}} \operatorname{sgn}(s_1) + \mu_2^2 s_1 \right] + \frac{d}{dt} w(t, \chi) \end{aligned} \quad (15)$$

Then, the candidate Lyapunov Function is defined as:

$$V(s_1, s_2, k_1, k_2) = V_0(\cdot) + \frac{1}{2\varsigma_1} (k_1 - k_1^*)^2 + \frac{1}{2\varsigma_2} (k_2 - k_2^*)^2 \quad (16)$$

where $\varsigma_1, \varsigma_2, k_1^*, k_2^*$ are positive constants and $V_0(\cdot)$ is given by:

$$V_0(s_1, s_2, k_1, k_2) = \xi^T P \xi \quad (17)$$

with:

$$\xi^T = [\phi_1(s_1), s_2] \quad (18)$$

and

$$P = P^T = \begin{bmatrix} \beta + 4\epsilon^2 & -2\epsilon \\ -2\epsilon & 1 \end{bmatrix} > 0 \quad (19)$$

Since β and ϵ are defined as an arbitrary positive constants, then P is a positive definite matrix. Moreover, note that the function $V_0(\cdot)$ satisfies the next form:

$$\lambda_{\min}(P) \|\xi\|_2^2 \leq V_0(s, k) \leq \lambda_{\max}(P) \|\xi\|_2^2 \quad (20)$$

where $\lambda_{\min}(P)$ and $\lambda_{\max}(P)$ are the smallest and greatest eigenvalue of P , respectively. $\|\xi\|_2^2 = |s_1| + 2|s_1|^{\frac{3}{2}} + s_1^2 + s_2^2$ is the Euclidean norm of ξ and the next inequality is satisfied as well:

$$|\phi(s_1)| \leq \|\xi\|_2 \leq \frac{V^{\frac{1}{2}}(\xi)}{\lambda_{\min}^{\frac{1}{2}}(P)} \quad (21)$$

213 Finally, it is important to note that the proposed candidate Lyapunov function
214 $V(s_1, s_2, k_1, k_2)$ is a continuous, positive definite and differentiable function.

215 The procedure to find the time derivative of the function $V(\cdot)$ is divided
216 into two main steps. First, the time derivative of $V_0(\cdot)$ is found. Second, the
217 total time derivative of $V(\cdot)$ is shown.

Step 1. Noting that $\phi_2(s_1) = \phi_1'(s_1)\phi_1(s_1)$, the derivative of $V_0(\cdot)$ is obtained as:

$$\dot{V}_0 = 2\xi^T P \dot{\xi} \quad (22)$$

$$= 2\xi^T P \begin{bmatrix} \phi_1' \left[-k_1\phi_1(s_1) + s_2 \right] \\ -k_2\phi_2(s_1) + \frac{d}{dt}w(t, \chi) \end{bmatrix} \quad (23)$$

$$= 2\xi^T P \begin{bmatrix} \phi_1'(s_1) \left[-k_1\phi_1(s_1) + s_2 \right] \\ \phi_1'(s_1)\phi_1(s_1) \left[-k_2 + L \right] \end{bmatrix} \quad (24)$$

$$= \phi_1'(s_1) 2\xi^T P \underbrace{\begin{bmatrix} -k_1 & s_2 \\ -(k_2 - L) & 0 \end{bmatrix}}_{A(t, \chi)} \xi \quad (25)$$

$$= \phi_1'(s_1) \xi^T (A^T(t, \chi)P + PA(t, \chi)) \xi \quad (26)$$

$$= -\phi_1'(s_1) \xi^T Q(t, \chi) \xi \quad (27)$$

where

$$Q(t, \chi) = \begin{bmatrix} 2k_1(\beta + 4\epsilon^2) - 4\epsilon(k_2 - L) & \star \\ k_2 - L - 2\epsilon k_1 - \beta - 4\epsilon^2 & 2\epsilon \end{bmatrix} \quad (28)$$

Selecting the gain $k_2 = 2\epsilon k_1 + \beta + 4\epsilon^2$, we have the following:

$$Q - 2\epsilon I = \begin{bmatrix} 2k_1\beta - 4\epsilon(\beta + 4\epsilon^2 - L) - 2\epsilon & -L \\ -L & 2\epsilon \end{bmatrix} \quad (29)$$

The matrix Q will be positive definite with a minimal eigenvalue $\lambda_{\min}(Q) \geq 2\epsilon$ if

$$k_1 > \delta_0 + \frac{\alpha_2^2}{4\epsilon\beta} + \frac{\epsilon \left[2(\beta + 4\epsilon^2 + L) + 1 \right]}{2\beta} \quad (30)$$

Then, the time derivative of $V_0(\cdot)$ can be rewritten as:

$$\dot{V}_0 = -\phi_1'(s_1)\xi^T Q(t, x)\xi \leq -2\epsilon\phi_1'(s_1)\xi^T \xi = -2\epsilon \left(\mu_1 \frac{1}{2|s_1|^{\frac{1}{2}}} + \mu_2 \right) \xi^T \xi \quad (31)$$

Finally, using (21), the time derivative of $V_0(\cdot)$ is expressed as:

$$\dot{V}_0 \leq -\frac{\epsilon\lambda_{\min}^{\frac{1}{2}}(P)}{\lambda_{\max}(P)}\mu_1 V_0^{\frac{1}{2}}(s, k) - \frac{2\epsilon}{\lambda_{\max}(P)}\mu_2 V(s, k) \quad (32)$$

$$\leq -\gamma V_0^{\frac{1}{2}}(s, k) \quad (33)$$

218 with $\gamma = \mu_1 \frac{\epsilon\lambda_{\min}^{\frac{1}{2}}(P)}{\lambda_{\max}(P)}$.

Step 2. The time derivate of the Lyapunov function (16) is given by:

$$\dot{V} = \dot{V}_0(\cdot) + \frac{1}{\varsigma_1}(k_1 - k_1^*)\dot{k}_1 + \frac{1}{\varsigma_2}(k_2 - k_2^*)\dot{k}_2 \quad (34)$$

$$\leq -\gamma V_0^{\frac{1}{2}}(s, k) + \frac{1}{\varsigma_1}(k_1 - k_1^*)\dot{k}_1 + \frac{1}{\varsigma_2}(k_2 - k_2^*)\dot{k}_2 \quad (35)$$

$$= -\gamma V_0^{\frac{1}{2}}(s, k) - \frac{\omega_1}{\sqrt{2\varsigma_1}}|k_1 - k_1^*| - \frac{\omega_2}{\sqrt{2\varsigma_2}}|k_2 - k_2^*| + \frac{1}{\varsigma_1}(k_1 - k_1^*)\dot{k}_1 + \quad (36)$$

$$+ \frac{1}{\varsigma_2}(k_2 - k_2^*)\dot{k}_2 + \frac{\omega_1}{\sqrt{2\varsigma_1}}|k_1 - k_1^*| + \frac{\omega_2}{\sqrt{2\varsigma_2}}|k_2 - k_2^*| \quad (37)$$

Using the Cauchy-Schwarz inequality, the first three terms of \dot{V} can be synthesized as follows:

$$-\gamma V_0^{\frac{1}{2}}(s, k) - \frac{\omega_1}{\sqrt{2\varsigma_1}}|k_1 - k_1^*| - \frac{\omega_2}{\sqrt{2\varsigma_2}}|k_2 - k_2^*| \leq -\pi\sqrt{V(s, k_1, k_2)} \quad (38)$$

219 where $\pi = \min(\gamma, \omega_1, \omega_2)$.

Assuming that there exist positive constants k_1^* and k_2^* such that $k_1 - k_1^* < 0$ and $k_2 - k_2^* < 0$ are satisfied $\forall t \geq 0$. Then, the time derivative of V can be rewritten as:

$$\begin{aligned}\dot{V} &\leq -\pi\sqrt{V(s, k_1, k_2)} - |k_1 - k_1^*| \left(\frac{1}{\varsigma_1} \dot{k}_1 - \frac{\omega_1}{\sqrt{2\varsigma_1}} \right) - |k_2 - k_2^*| \left(\frac{1}{\varsigma_2} \dot{k}_2 - \frac{\omega_2}{\sqrt{2\varsigma_2}} \right) \\ &= -\pi\sqrt{V(s, k_1, k_2)} + \vartheta\end{aligned}\quad (39)$$

where:

$$\vartheta = -|k_1 - k_1^*| \left(\frac{1}{\varsigma_1} \dot{k}_1 - \frac{\omega_1}{\sqrt{2\varsigma_1}} \right) - |k_2 - k_2^*| \left(\frac{1}{\varsigma_2} \dot{k}_2 - \frac{\omega_2}{\sqrt{2\varsigma_2}} \right)\quad (40)$$

In order to preserve the finite time convergence it is necessary assure the condition $\vartheta = 0$ which will be achieved through the adaption gain laws as follows:

$$\dot{k}_1 = \omega_1 \sqrt{\frac{\varsigma_1}{2}}\quad (41)$$

$$\dot{k}_2 = \omega_2 \sqrt{\frac{\varsigma_2}{2}}\quad (42)$$

220 In brief, the adaptive gains k_1 and k_2 will be increase based on the dynamic
 221 and algebraic equations stated in (12) until the condition (30) is reached.
 222 Then, the matrix Q will be positive definite and the finite time convergence
 223 will be assured according to (39). Finally, when the sliding variable σ and its
 224 derivative converges to zero, the adaptive gains k_1 and k_2 will stop growing
 225 by making $\dot{k}_1 = 0$ as $\sigma = 0$. Subsequently, it is obtained the gain-adaptation
 226 law (12).

227 4. Real-Time Experimental Results

228 To demonstrate the practical feasibility of the developed controller, we
 229 applied the control algorithm to *Leonard* ROV (see Fig. 3), which is an
 230 underwater vehicle developed at the LIRMM (CNRS/University Montpellier,
 231 France). *Leonard* is a tethered underwater vehicle which is $75 \times 55 \times 45$ cm
 232 in dimension and 28 kg in weight. The propulsion system of this vehicle
 233 consists of six thrusters to obtain a fully actuated system.

234 The underwater robot is driven by a laptop computer, with CPU Intel
 235 Core i7-3520M 2.9 GHz, 8GB of RAM. The computer runs under Windows

236 7 operating system, and the control software is developed with Visual C++
 237 2010. The computer receives the data from the ROV's sensors (pressure,
 238 IMU), computes the control laws and sends input signals to the actuators.
 239 Syren 25 Motor Drives control these latter. The main features of this vehicle
 are described in Table 1. The control algorithm was experimentally tested in

Mass	28 <i>kg</i>
Buoyancy	9 <i>N</i>
Dimensions	75 × 45 cm
Maximal depth	100m
Thrusters	6 Seabotix BTD150
Power	48V - 600 W
Attitude Sensor	Sparkfun Arduimu V3 Invensense MPU-6000 MEMS 3-axis gyro and accelerometer 3-axis I2C magnetometer HMC-5883L Atmega328 microprocessor
Camera	Pacific Co. VPC-895A CCD1/3 PAL-25-fps
Depth sensor	Preasure Sensor Breakout-MS5803-14BA
Sampling period	40 ms
Surface computer	Dell Latitude E6230- Intel Core i7 -2.9 GHz Windows 7 Professional 64 bits Microsoft Visual C++ 2010
Tether length	150 m

Table 1: Main Features of the underwater vehicle

240
 241 the $4 \times 4 \times 1.2$ m pool of the LIRMM (see Fig. 11). Although the proposed
 242 control law was given by (10) is designed for the whole system of six degrees
 243 of freedom, the real-time experiments shown in this article concern only
 244 depth and yaw motions. The primary objective of the designed control law
 245 is to robustly track a desired trajectory in depth and yaw despite parameter
 246 uncertainties and external disturbances.

247 4.1. Proposed Scenarios and Technical Details

248 To test the robustness of the proposed controller, four different scenarios
 249 have been performed, namely:

- 250 1. Scenario 1: Nominal case.
 251 In this scenario, the AUV follows the desired trajectory in depth and
 252 yaw simultaneously in the absence of external disturbances or paramet-
 253 ric uncertainties. During this test, the controller’s gains are adjusted to
 254 obtain the best tracking performance. These gains remain unchanged
 255 during all the remaining experiments.
- 256 2. Scenario 2: Robustness towards parametric uncertainties.
 257 In this test, the buoyancy and damping of the vehicle were modified
 258 to test the effectiveness of the controller and its robustness towards
 259 parametric uncertainties.
- 260 3. Scenario 3: Robustness towards external disturbances.
 261 This test was inspired by a more realistic scenario, where the vehicle
 262 has the task of loading an object and when reaching a certain depth,
 263 dropping that object. In this test, it is possible to observe a sudden
 264 change in the vehicle’s weight and how it affects the controller perfor-
 265 mance.
- 266 4. Scenario 4: Robustness towards disturbances in the control law.
 267 In this experiment, the controller was perturbed though an aggressive
 268 disturbance generated by software to show the advantages of the adap-
 269 tive algorithm towards persistent disturbances.

270 During the listed experiments, the adaptive controller was compared against
 271 the GSTA nominal design with constant gains to show the improvements
 272 of the proposed controller. The GSTA was tuned heuristically but always
 273 considering the constraints given by the stability proofs shown in [28]. For
 274 example, the GSTA could be seen as a kind of nonlinear PI controller and
 275 the tuning procedure is enclosed as follows:

- 276 1. Fix the values $\mu_{1i} = \mu_{2i} = 1$, $\Lambda_i = 1$ and $k_{23} = 0.0001$ and the gain k_{1i}
 277 is increased until the controller reaches the desired value and starts to
 278 oscillate.
- 279 2. Decrease a fraction of k_{1i} and then increase the value of k_{23} slightly
 280 until the oscillation in steady state decrease.
- 281 3. The rate of convergence to the desired signal is modified through the
 282 value of Λ_i .

283 In order to prevent the chattering effect in the GSTA control input, it is
 284 suggested to keep the gain k_{2i} in a small value. After tuning the algorithm
 285 for a constant reference, the control law was tested for a trajectory tracking

286 task without considering external disturbances (nominal case), where the
 287 values of the gains were improved until reach a good performance and can
 288 be seen in Table 2.

289 The tuning process of the adaptive controller is summarized in the fol-
 290 lowing steps:

- 291 1. Using the values of μ_{1i} , μ_{2i} and Λ_i found in the previous case, fix the
 292 values $\varsigma_i = 1$ and $\omega_i = 0.01$. To modify the convergence velocity to the
 293 set-point, the parameter ω_i need to be increased.
- 294 2. Fix the parameters $\epsilon_i = 0.01$ and $\beta_i = 0.01$. Then, slightly increase
 295 the value of one of the two mentioned parameters until oscillations in
 296 steady-state decrease.

297 The chosen parameters are shown in Table 3.

Finally, it is necessary to emphasize that the gains of the adaptive con-
 troller shown in equation (12) depend directly over the sliding surface $\sigma(t)$.
 Moreover, $\sigma(t)$ is related to the underwater vehicle system state η as stated
 in (9). In practice, sensors which provide the data η , supply noisy measure-
 ments. Thus, the condition $\sigma(t) = 0$ is not realistic and never satisfied which
 leads to a steady growth of the controller gains $k_1(t)$ and $k_2(t)$. To overcome
 the mentioned drawback, the condition (12) is modified as follows:

$$k_{1i}(t) = \begin{cases} 0 & \text{if } -\epsilon_i \leq \sigma \leq \epsilon_i \\ \mu_{1i}\sqrt{\frac{\varsigma_{1i}}{2}} & \text{otherwise} \end{cases} \quad (43)$$

$$k_{2i}(t) = 2\epsilon_i k_{1i}(t) + \beta_i + 4\epsilon_i^2 \quad (44)$$

where ϵ is a small positive parameter.

Depth	$k_{13} = 0.30$	$k_{23} = 0.005$	$\Lambda_3 = 2.5$
Yaw	$k_{16} = 2.0$	$k_{26} = 0.15$	$\Lambda_6 = 6.0$

Table 2: GSTA controller gains used in real-time experiments

298

299 4.2. Control in nominal conditions

300 The upper plot of Figure 2 shows the depth and yaw tracking controller
 301 performance of the robot during the first case. In this experiment, the vehicle
 302 follows a trajectory in depth going from the surface to a maximal depth of
 303 30 cm, where the vehicle remains stable in that position for 20 seconds and

Depth	$\mu_3 = 0.1$	$\varsigma_3 = 1.0$	$\Lambda_3 = 2.5$
	$\epsilon_3 = 0.01$	$\beta_3 = 0.035$	$\varepsilon_3 = 0.1$
Yaw	$\mu_6 = 0.3$	$\varsigma_6 = 1.0$	$\Lambda_6 = 6.0$
	$\epsilon_6 = 0.01$	$\beta_6 = 0.10$	$\varepsilon_6 = 0.1$

Table 3: Adaptive control gains used in real-time experiments

Scenario	Adaptive		GSTA	
	$RMSE_z$ [m]	$RMSE_\psi$ [deg]	$RMSE_z$ [m]	$RMSE_\psi$ [deg]
	Depth	Yaw	Depth	Yaw
1	0.0013	0.2077	0.0027	0.2872
2	0.0196	0.1758	0.0897	0.6375
3	0.0200	0.1147	0.0648	0.3063
4	0.0101	1.2541	0.0713	2.6987

Table 4: Control gains used in real-time experiments

304 finally emerges to 20 cm and hovers until the trial ends. For the yaw motion,
 305 the vehicle turns from its initial position to 60 degrees in 6 seconds. Then, it
 306 remains stable in that position for 20 seconds. Finally, the robot goes to -60
 307 degrees and stay there until the test ends. It can be noticed that the GSTA
 308 controller takes a short lapse of time to converge to the reference while the
 309 adaptive version takes about 15 seconds to converge to the reference signal.
 310 This behavior can be explained because the gains of the adaptive controller
 311 are selected by a dynamic equation which is updating itself depending on
 312 the sliding surface σ value. When the value of σ is far from zero, the gains
 313 of the adaptive algorithm is increased until the condition (30) is reached.
 314 Besides, the tracking error evolution is shown in the middle of Figure 2
 315 and can be analyzed through numerical data of Root Mean Square Error
 316 (RMSE) which is displayed in Table 4. The numerical results of Table 4
 317 show an improvement of the adaptive controller over the nominal design.
 318 Also, the behavior of the control inputs is displayed at the bottom of Figure
 319 2. From this Figure, it can be noticed that the control signal of the adaptive
 320 controller is smoother than the control signal of the nominal GSTA. Finally,
 321 the evolution of the adaptive controller gains is shown in Figure 3.

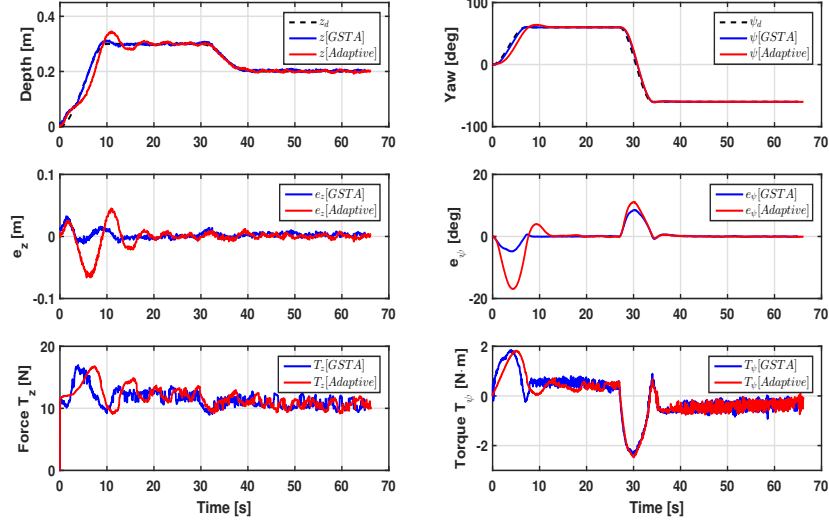


Figure 2: Performance comparison of the GSTA (blue line) and the adaptive GSTA (red line). (Upper) Trajectory tracking in depth and yaw in absence of disturbances. (Middle) Plots of the error signal. (Lower) Evolution of the control inputs.

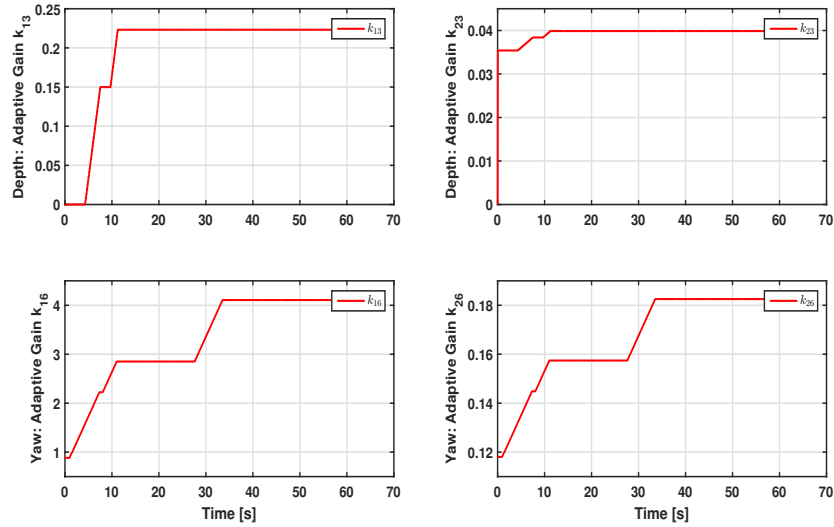


Figure 3: Evolution of the adaptive controller gains. (Upper) Updating of the gains for depth trajectory tracking. (Lower) Evolution of the gains for the yaw trajectory tracking test.

322 4.3. Control towards parametric uncertainties

323 To evaluate the robustness of the proposed controller against parametric
324 uncertainties, the buoyancy of the vehicle was modified by tying two floats
325 to the sides of the robot, increasing the floatability by 200%. To modify the
326 damping of the submarine, a large rigid sheet of plastic that has a dimension
327 of 45×10 cm was attached on one side of the vehicle, increasing the rotational
328 damping along the z-axis by approximately 90%.

329 The trajectory tracking for depth and yaw motion is shown in the top of
330 Figure 4. On the one hand, due to the large persistent disturbance in heave
331 motion, the nominal GSTA controller is not capable of following the depth
332 reference signal. On the other hand, the adaptive GSTA only takes about 15
333 seconds to converge to the reference depth trajectory despite the parametric
334 disturbance in heave motion. Furthermore, the behavior of both controllers
335 is similar during the yaw trajectory tracking test. The plot of the tracking
336 errors is displayed in the middle of Figure 4. It should be noted the fast
337 convergence of the adaptive algorithm over the nominal design performance.
338 As mentioned before, the tracking in yaw is similar for both cases. The RMSE
339 for the controller's couple is summarized in Table 4. As in the nominal
340 case, the improvement of the adaptive version over the nominal GSTA is
341 demonstrated through numerical data. Also, in the bottom of Figure 4 we
342 can observe the progress of the control inputs. For example, for the depth
343 following, we can observe that the force increases almost twice compared with
344 the nominal case, this suggests that there is a strong compromise between
345 the controller's ability to reject disturbances with the increase in energy that
346 is demanded from the actuators. Finally, the evolution of the adaptive gains
347 of the GSTA is shown in Figure 5. It is important to note that the gains
348 update itself every time that the robot submerges, emerges or turns.

349 4.4. Control towards external disturbances

350 In some applications, underwater vehicles are equipped with robotic ma-
351 nipulators which allow to carry objects and take them to a specific depth or
352 pick them up from the ocean floor to transport them to the surface. That
353 practical case inspires this scenario, to simulate that the robot carries a load,
354 a metallic block of 1 kg was tied to the submarine with a rope of a length
355 about 20 cm. In this scenario, the maximal depth of the reference trajectory
356 was set at 40 cm. Regarding the maximum depth of the basin is 50 cm, the
357 robot will be suddenly disturbed when it reaches 30 centimeters, because the
358 metallic block will touch the floor, thus suddenly canceling its weight's effect.

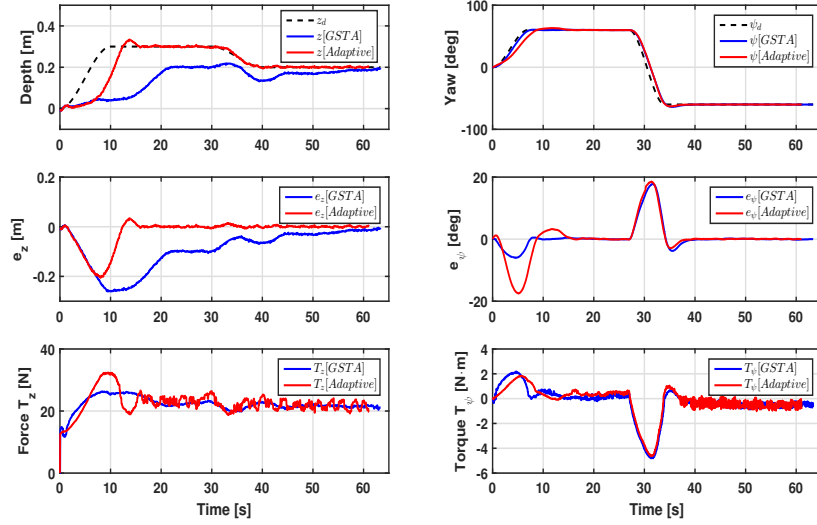


Figure 4: Robustness of the GSTA (blue line) and the Adaptive GSTA (red line) controller performance towards parametric uncertainties. The floatability of the submarine was increased 200% while the damping along z-axis was modify up to 90% respect the nominal case.

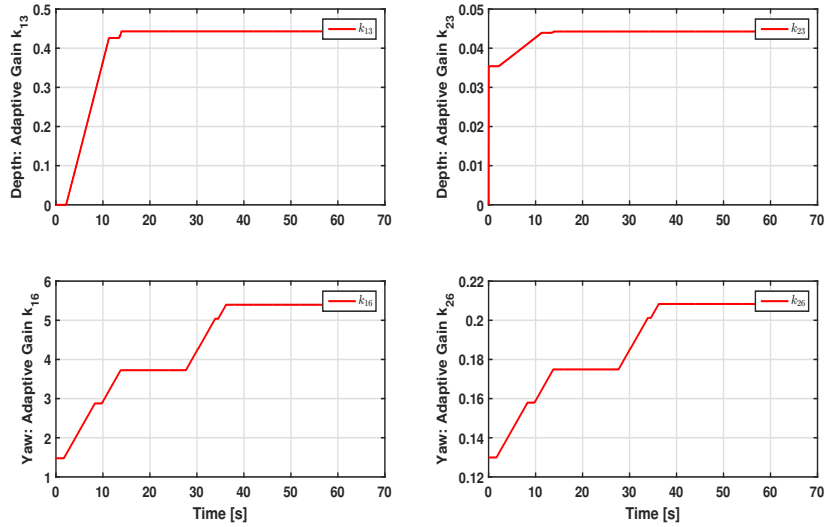


Figure 5: Evolution of the adaptive controller gains. (Upper) Updating of the gains for depth trajectory tracking. (Lower) Evolution of the gains for the yaw trajectory tracking test.

359 The disturbance will be acting on the robot until it starts to emerge and it
360 reaches 30 cm, the action of the extra weight will influence the trajectory of
361 the submarine again (see Figure 6).

362 The results of the controller’s performance in the robustness test against
363 external disturbances are shown in Figure 7. At the top of the graph, the ini-
364 tial position of the vehicle is at 30 cm deep due to the influence of the added
365 extra weight. When the test begins, the robot reaches the desired trajectory
366 in about 5 and 15 seconds under the nominal GSTA and the adaptive con-
367 troller, respectively. In the 10th second, the 1kg block touches the floor, and
368 the total weight of the vehicle suddenly changes. Both controllers are capable
369 of compensating the effect of the disturbance some seconds later. When the
370 vehicle emerges, the extra weight acts again on the submarine degrading the
371 trajectory tracking. While the nominal GSTA cannot compensate the distur-
372 bance’s effect, the adaptive algorithm counteracts the perturbation impact,
373 and the submarine converges to the reference signal accurately. The error
374 plots are displayed at the middle of Figure 7, while the numerical value of
375 the RMSE is shown in Table 4. The control input signals are shown at the
376 bottom of Figure 7. Finally, the evolution of the adaptive controller gains is
377 shown in Figure 8.

378 4.5. Control signal disturbed by software

379 Most of the commercial underwater vehicles have two maneuvering modes:
380 ROV and Autonomous mode. When the vehicle is performing a task au-
381 tonomously, and a mechanical failure or a wrong behavior occurs, the ve-
382 hicle’s operator can switch from one mode to another in order to prevent
383 damage to the environment or the vehicle itself. Switching from one mode
384 to another can take a few seconds if the vehicle is performing a mission at
385 considerable depth and suddenly an actuator’s drives fail, then, a few seconds
386 could represent a big issue because the operator can lose the robot. Based on
387 the mentioned scenario, while the underwater vehicle is performing the tra-
388 jectory tracking as in the same conditions as in the nominal case, a constant
389 signal (see Figure X) is introduced to the robot control input to simulate a
390 failure in the actuator’s driver.

391 The tracking trajectory for depth and yaw is shown in the upper part of
392 Figure 9. From the tracking in depth, it can be noted that both controllers
393 have the same rate of convergence as in the nominal case. However, the per-
394 formance of the nominal GSTA is highly degraded when the simulated failure
395 on the robot actuator appears while the Adaptive controller can compensate

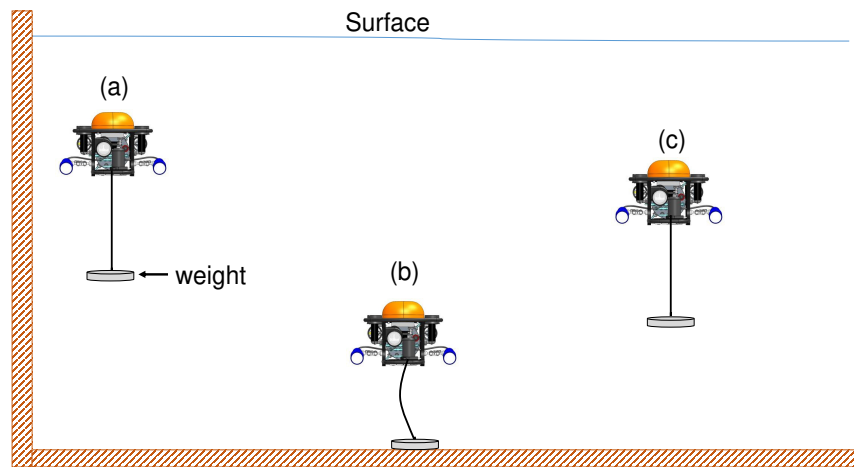


Figure 6: Description of the robustness towards external disturbances test. (a) 1 kg weight is attached to the submarine, (b) the action of the extra weight disappears when the vehicle reaches 30 cm in depth. Again, the robot is disturbed by the weight when the vehicle emerges (c).

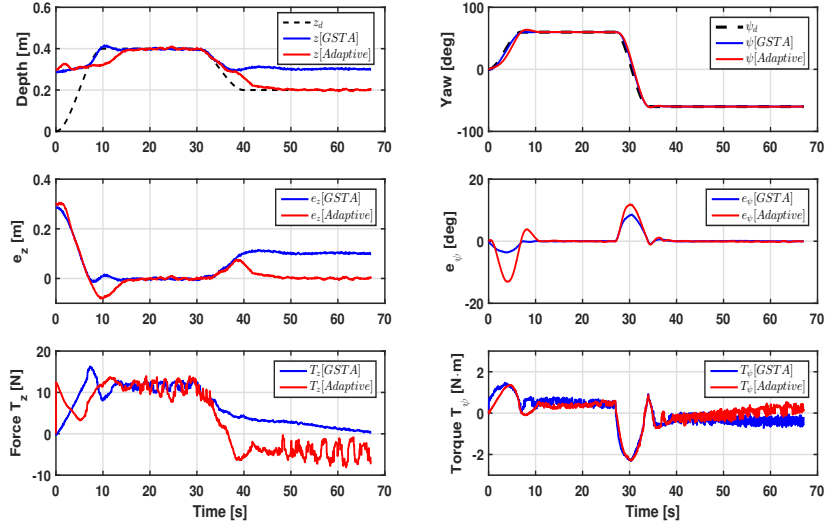


Figure 7: Performance of the proposed controller towards external disturbances test. (Upper) Trajectory tracking in depth and yaw: The 1 kg block is attached to the submarine which produced disturbances at 8 and 35 seconds when the block touches and takes off the floor, respectively. (Middle) Plots of the error signal. (Lower) Evolution of the control inputs.

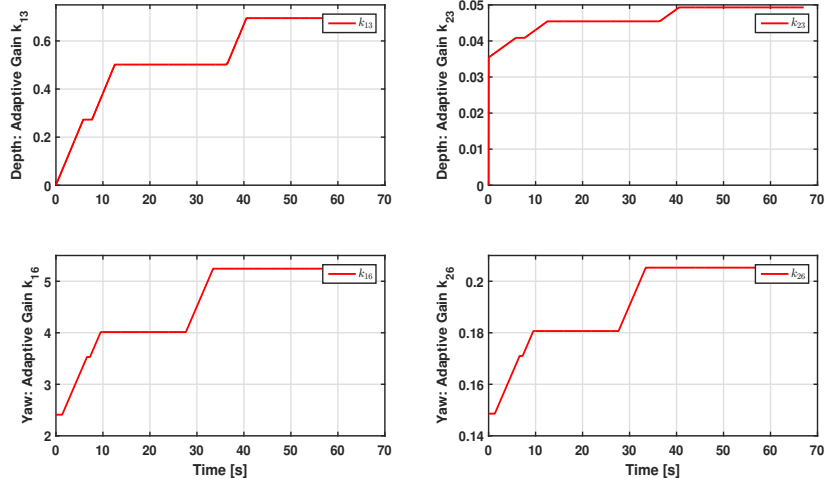


Figure 8: Evolution of the adaptive controller gains. (Upper) Updating of the gains for depth trajectory tracking. (Lower) Evolution of the gains for the yaw trajectory tracking test.

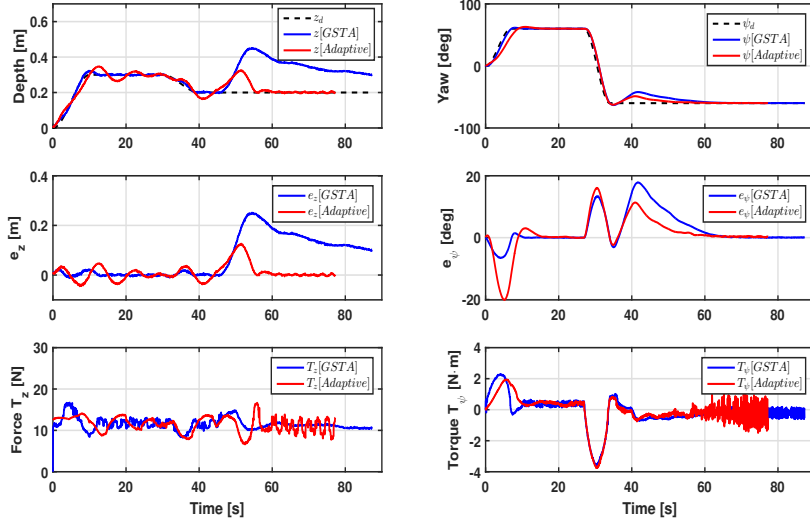


Figure 9: Underwater Vehicle actuators failure test: A large signal is introduced to the input signal acting as a disturbance at 45th second. (Upper) Trajectory tracking in depth and yaw of the GSTA (blue line) and the adaptive controller (red line). (Middle) Plots of the error signal. (Lower) Evolution of the control inputs.

396 the disturbance fast. On the other hand, the yaw tracking test shows again
 397 that the adaptive control performance is superior compared over the GSTA
 398 with constant gains.

399 In the middle of Figure 9, the plot of errors are depicted and the improve-
 400 ment of each controller is visually apparent and can be confirmed numerically
 401 through the RMSE Table 4. Also, the control inputs are displayed at the
 402 bottom of Figure 9. From this part of the Figure, it is worth to observe that
 403 there is a trade-off between the adaptive controller ability to reject large
 404 constant disturbances and the high controller gains. It means, based on the
 405 dynamic equation to select the controller gains, larges disturbances will be
 406 attenuated by high values of k_1 and k_2 . Finally, the evolution of the adaptive
 407 controller gains is shown in Figure 10. Is interesting observe how the gains
 408 are increased when the disturbance is introduced into the control input.

409 5. Conclusions

410 In this paper, an decoupled adaptive high order sliding mode control
 411 has been developed for trajectory tracking control of an autonomous under-

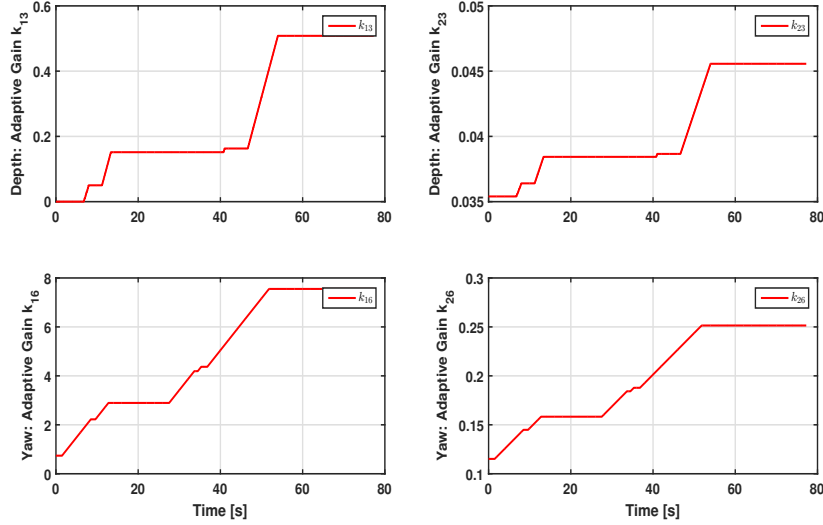


Figure 10: Evolution of the adaptive controller gains. Updating of the gains for depth trajectory tracking (Upper) and the yaw trajectory tracking control (Lower).

412 water vehicle. A Lyapunov design was proposed to prove the stability of
 413 the closed-loop system. The proposed controller has been implemented for
 414 trajectory tracking in depth and yaw motions on the LEONARD ROV un-
 415 derwater vehicle. The obtained real-time experimental results demonstrate
 416 the effectiveness and robustness of the proposed control law towards external
 417 disturbances and persistent parametric uncertainties.

418 Acknowledgment

419 This work was supported by Conacyt, grant 490978. The Leonard under-
 420 water vehicle has been financed by the European Union (FEDER grant n°
 421 49793) and the Region Occitanie (ARPE Pilot Plus project).

- 422 [1] Y. C. Sun, C. C. Cheah, Adaptive control schemes for autonomous
 423 underwater vehicle, *Robotica* 27 (2009) 119–129.
- 424 [2] S. Zhao, J. Yuh, Experimental study on advanced underwater robot
 425 control, *IEEE transactions on robotics* 21 (2005) 695–703.

- 426 [3] D. A. Smallwood, L. L. Whitcomb, Model-based dynamic positioning
427 of underwater robotic vehicles: theory and experiment, *IEEE Journal*
428 *of Oceanic Engineering* 29 (2004) 169–186.
- 429 [4] T. I. Fossen, *Guidance and control of ocean vehicles*, John Wiley & Sons
430 Inc, 1994.
- 431 [5] P. Herman, Decoupled pd set-point controller for underwater vehicles,
432 *Ocean Engineering* 36 (2009) 529–534.
- 433 [6] X. Xiang, C. Yu, L. Lapierre, J. Zhang, Q. Zhang, Survey on fuzzy-logic-
434 based guidance and control of marine surface vehicles and underwater
435 vehicles, *International Journal of Fuzzy Systems* 20 (2018) 572–586.
- 436 [7] M. H. Khodayari, S. Balochian, Modeling and control of autonomous
437 underwater vehicle (auv) in heading and depth attitude via self-adaptive
438 fuzzy pid controller, *Journal of Marine Science and Technology* 20 (2015)
439 559–578.
- 440 [8] R. Cui, C. Yang, Y. Li, S. Sharma, Adaptive neural network control
441 of auvs with control input nonlinearities using reinforcement learning,
442 *IEEE Transactions on Systems, Man, and Cybernetics: Systems* 47
443 (2017) 1019–1029.
- 444 [9] Z. Yan, M. Wang, J. Xu, Global adaptive neural network control of un-
445 deractuated autonomous underwater vehicles with parametric modeling
446 uncertainty, *Asian Journal of Control* (2019).
- 447 [10] C. Shen, Y. Shi, B. Buckham, Trajectory tracking control of an au-
448 tonomous underwater vehicle using lyapunov-based model predictive
449 control, *IEEE Transactions on Industrial Electronics* 65 (2018) 5796–
450 5805.
- 451 [11] J.-H. Li, P.-M. Lee, Design of an adaptive nonlinear controller for depth
452 control of an autonomous underwater vehicle, *Ocean engineering* 32
453 (2005) 2165–2181.
- 454 [12] L. G. García-Valdovinos, T. Salgado-Jiménez, M. Bandala-Sánchez,
455 L. Nava-Balanzar, R. Hernández-Alvarado, J. A. Cruz-Ledesma, Mod-
456 elling, design and robust control of a remotely operated underwater ve-
457 hicle, *International Journal of Advanced Robotic Systems* 11 (2014)
458 1.

- 459 [13] H. Joe, M. Kim, S.-c. Yu, Second-order sliding-mode controller for au-
460 tonomous underwater vehicle in the presence of unknown disturbances,
461 *Nonlinear Dynamics* 78 (2014) 183–196.
- 462 [14] Z. H. Ismail, V. W. Putranti, Second order sliding mode control scheme
463 for an autonomous underwater vehicle with dynamic region concept,
464 *Mathematical Problems in Engineering* 2015 (2015).
- 465 [15] I. D. Landau, R. Lozano, M. M'Saad, A. Karimi, *Adaptive control: al-*
466 *gorithms, analysis and applications*, Springer Science & Business Media,
467 2011.
- 468 [16] Y. Shtessel, C. Edwards, L. Fridman, A. Levant, *Sliding mode control*
469 *and observation*, volume 10, Springer, 2014.
- 470 [17] T. Gonzalez, J. A. Moreno, L. Fridman, Variable gain super-twisting
471 sliding mode control, *IEEE Transactions on Automatic Control* 57
472 (2012) 2100–2105.
- 473 [18] Y. Shtessel, M. Taleb, F. Plestan, A novel adaptive-gain supertwisting
474 sliding mode controller: Methodology and application, *Automatica* 48
475 (2012) 759–769.
- 476 [19] N. Q. Hoang, E. Kreuzer, A robust adaptive sliding mode controller for
477 remotely operated vehicles, *Technische Mechanik* 28 (2008) 185–193.
- 478 [20] R. Cui, X. Zhang, D. Cui, Adaptive sliding-mode attitude control for
479 autonomous underwater vehicles with input nonlinearities, *Ocean En-*
480 *gineering* 123 (2016) 45–54.
- 481 [21] Z. Chu, D. Zhu, S. X. Yang, G. E. Jan, Adaptive sliding mode control
482 for depth trajectory tracking of remotely operated vehicle with thruster
483 nonlinearity, *The Journal of Navigation* 70 (2017) 149–164.
- 484 [22] G.-c. Zhang, H. Huang, L. Wan, Y.-m. Li, J. Cao, Y.-m. Su, et al., A
485 novel adaptive second order sliding mode path following control for a
486 portable auv, *Ocean Engineering* 151 (2018) 82–92.
- 487 [23] Y. Wang, L. Gu, M. Gao, K. Zhu, Multivariable output feedback adap-
488 tive terminal sliding mode control for underwater vehicles, *Asian Journal*
489 *of Control* 18 (2016) 247–265.

- 490 [24] L. Qiao, W. Zhang, Adaptive second-order fast nonsingular terminal
491 sliding mode tracking control for fully actuated autonomous underwater
492 vehicles, *IEEE Journal of Oceanic Engineering* (2018).
- 493 [25] M. Sarfraz, F. u. Rehman, I. Shah, Robust stabilizing control of nonholo-
494 nomic systems with uncertainties via adaptive integral sliding mode: An
495 underwater vehicle example, *International Journal of Advanced Robotic
496 Systems* 14 (2017) 1729881417732693.
- 497 [26] A. Levant, Sliding order and sliding accuracy in sliding mode control,
498 *International journal of control* 58 (1993) 1247–1263.
- 499 [27] Y. B. Shtessel, J. A. Moreno, F. Plestan, L. M. Fridman, A. S. Poznyak,
500 Super-twisting adaptive sliding mode control: A lyapunov design, in:
501 *Decision and Control (CDC), 2010 49th IEEE Conference on, IEEE*, pp.
502 5109–5113.
- 503 [28] J. A. Moreno, A linear framework for the robust stability analysis of a
504 generalized super-twisting algorithm, in: *Electrical Engineering, Com-
505 puting Science and Automatic Control, CCE, 2009 6th International
506 Conference on, IEEE*, pp. 1–6.
- 507 [29] K. D. Do, J. Pan, *Control of ships and underwater vehicles: design
508 for underactuated and nonlinear marine systems*, Springer Science &
509 Business Media, 2009.
- 510 [30] G. Antonelli, T. I. Fossen, D. R. Yoerger, Underwater robotics, in:
511 *Springer handbook of robotics*, Springer, 2008, pp. 987–1008.
- 512 [31] T. T. J. Presterro, Verification of a six-degree of freedom simulation
513 model for the REMUS autonomous underwater vehicle, Ph.D. thesis,
514 Massachusetts institute of technology, 2001.
- 515 [32] J. Vervoort, Modeling and control of an unmanned underwater vehicle,
516 Ph.D. thesis, Ph. D. thesis, University of Canterbury, 2009.
- 517 [33] S. of Naval Architects, M. E. U. Technical, R. C. H. Subcommittee,
518 *Nomenclature for Treating the Motion of a Submerged Body Through a
519 Fluid: Report of the American Towing Tank Conference*, Technical and
520 research bulletin, Society of Naval Architects and Marine Engineers,
521 1950.